

Alignment and Test of the Wide Field Infrared Survey Telescope (WFIRST) Engineering Design Unit (EDU) Grism

John Hagopian^a, Josh Berrier^a, John Chambers^b, David Content^b, Margaret Dominguez^b, Qian Gong^b, Jason Krom^a, Catherine Marx^b, Joseph McMann^c, Bert Pasquale^b, Laurie Seide^d, Arthur Whipple^e, Patrick Williams^d

^a ATA Aerospace, Albuquerque, NM 87123

^b NASA Goddard Space Flight Center, 8800 Greenbelt Road, Greenbelt, MD, USA 20771

^c Sierra Lobo, Sanduskey, OH

^d KBR Government Solutions, Greenbelt, MD 20770

^e Conceptual Analytics, LLC, Glenn Dale, MD, USA 20769

ABSTRACT

The WFIRST wide field instrument (WFI) includes a slitless spectrometer, which plays an important role in the WFIRST mission for the survey of emission-line galaxies. WFI is building engineering design and environmental test (EDU and ETU) units to reduce risk for the flight grism unit. We report here on successful build and test of the EDU grism. The four-element EDU grism consists of two prism elements and two diffractive elements that provide R700 dispersion. The elements were fabricated with alignment fiducials and integral flats to allow opto-mechanical alignment in six-degrees of freedom. Each element in turn, was installed onto a hexapod and positioned to its nominal orientation relative to the grism deck, then bonded into individual cells. Alignment measurements were performed in situ using theodolites to set tip/tilt and a Micro-vu non-contact Multisensor Measurement System was used to set despace, decenter and clocking of each element using the hexapod. After opto-mechanical alignment, the grism wavefront was measured using an Infrared ZYGO interferometer at various field points extending over a 20 by 14-degree (local) field of view. Using modeled alignment sensitivities, we determined the alignment correction required on our Element 2 prism compensator and successfully minimized the field dependent wavefront error and confocality. This paper details the alignment and testing of the EDU grism at ambient and cold operating temperatures.

Keywords: WFIRST, grism, slitless spectrometer,

1. INTRODUCTION

The Wide-Field Infrared Survey Telescope (WFIRST) is a NASA observatory designed to perform wide-field imaging and slitless spectroscopic surveys of the near infrared (NIR) sky for the community.¹ The current WFIRST design of the mission makes use of an existing 2.4m diameter telescope to enhance sensitivity and imaging performance. The WFIRST payload includes two main instruments: a Wide Field Instrument (WFI) and a Coronagraph Instrument (CGI). The WFI provides the wide-field imaging and slitless spectroscopy capability required to perform the dark energy, exoplanet microlensing, and NIR surveys. A compound grism design is selected for slitless spectroscopy. More specifically, the slitless spectroscopy is going to survey the emission-line galaxies to cover red-shift $1 < z < 6$ (Figure 1).] The purpose of the Engineering Design Unit Grism is to demonstrate the ability to align the four element grism and achieve the required wavefront quality across the large field of view and at 170K operating temperature. A Prototype grism² built in pre-phase A demonstrated on-axis wavefront quality and spectral resolution but did not achieve the desired performance off-axis. A different approach was used on the EDU whereby each element was fiducialized to allow deterministic alignment, which was followed by wavefront mapping across the field of view. Optical modeling determined that the resulting wavefront error could be optimized by adjustment of a single compensator element. The EDU grism met its

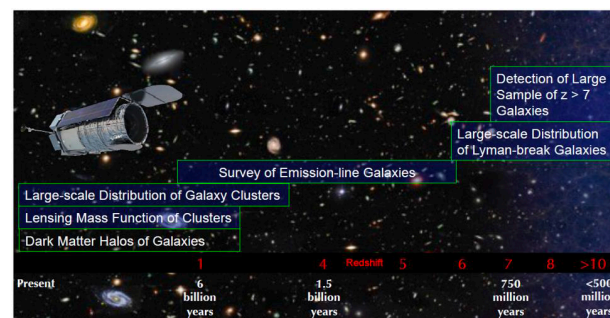


Figure 1. WFIRST: Probe of cosmic structure formation history.

going to survey the emission-line galaxies to cover red-shift $1 < z < 6$ (Figure 1).] The purpose of the Engineering Design Unit Grism is to demonstrate the ability to align the four element grism and achieve the required wavefront quality across the large field of view and at 170K operating temperature. A Prototype grism² built in pre-phase A demonstrated on-axis wavefront quality and spectral resolution but did not achieve the desired performance off-axis. A different approach was used on the EDU whereby each element was fiducialized to allow deterministic alignment, which was followed by wavefront mapping across the field of view. Optical modeling determined that the resulting wavefront error could be optimized by adjustment of a single compensator element. The EDU grism met its

performance requirements on and off-axis and at cold operating temperatures. This paper summarizes the successful alignment, modeling and testing of the EDU grism wavefront error at its center wavelength of 1550 nm.

2. OPTICAL DESIGN OF GRISM ASSEMBLY

2.1 Optical Design of EDU Grism

The EDU Grism assembly is a four-element design, including two powered prisms and two flat diffractive elements. Each of the diffractive elements has one diffractive surface on it. The reason for adding the second diffractive surface is that a grating in a non-collimated space introduces a lot of aberration. This aberration is not only a function of incident angle, but also linear to the wavelength. It is not possible to compensate the aberration scaled to wavelength using conventional optics, even when freeform aspheric surfaces are used. Since aberrations created from diffractive surfaces are all scaled to wavelength, adding another diffractive surface to compensate the aberration created by the 1st diffractive surface becomes a natural solution for this grism design. The patterns on both diffractive surfaces are curved variable spacing gratings. They provided a near perfect compensation from 1000 – 1900 nm wavelength range for the wide field of view. The main function of the two powered prisms that are sandwiched between the diffractive elements is to produce zero deviation for the central wavelength. It also helps to make the total assembly zero defocus in the telescope $\sim f/8$ beam. All surfaces of the powered prisms are spherical. The material is Suprasil IR grade fused silica for all four grism elements. The whole assembly is compact in order to fit into very limited space. Figure 2. shows the EDU grism optical design; the elements E1- E4 are approximately 125 mm in diameter.

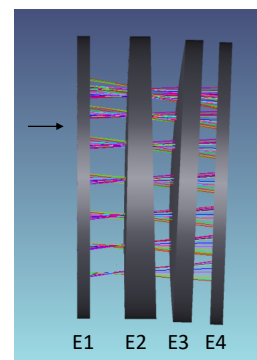


Figure 2. EDU Grism Optics

2.2 Grism Mechanical Design

The grism mechanical design is challenging due to the small package, requirements for alignment, cooldown stability and robustness for vibration qualification. The optical and mechanical team collaborated to define requirements for the grism assembly and post assembly alignment. The grism mechanical design shown in Figure 3, accommodates a variety of alignment references, including alignment cubes on the deck and each element cell as well as nests for spherically mounted retroreflectors (SMR's) or tooling balls used for laser tracker or laser radar measurements. The grism design allows for alignment adjustment of elements 2 through 4 in tip/tilt and despace by shimming at three spherical washer interfaces for post assembly optimization. During

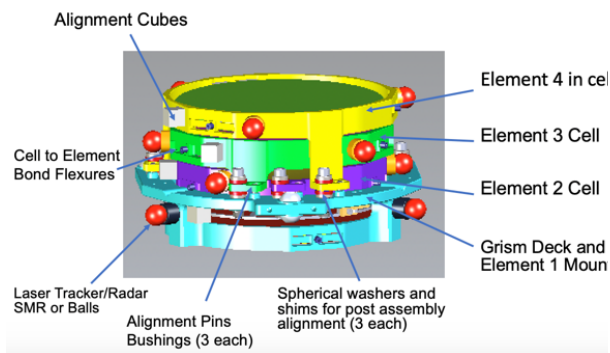


Figure 3. EDU Grism Mechanical Assembly

assembly the elements are aligned to the grism mount local coordinate system in 6-degrees of freedom using metrology and a hexapod to place them accurately in their cells before bonding them. Optical modeling indicates that our assembly tolerances should be good enough to allow optimization using only tip/tilt of our selected alignment compensator, E2. Since the elements are aligned one at a time in their cells during assembly and then removed we employ alignment pins on the mount that are registered to holes on the cells using alignment bushings to allow repeatable decenter and clocking alignment of the cells to the mount. The elements are all Suprasil; an infrared optimized variety of fused silica, which has a coefficient of thermal expansion that matches closely with the invar deck and cells. This allows for minimum alignment shift and cooldown strain to the operating temperature of the grism of 170 Kelvins and its survival temperature of 120 Kelvins. The grism also has to maintain its performance through a vibration test that simulates the launch environment of the WFIRST Observatory.

2.3 Grism Element Fabrication and Fiducialization

The EDU diffractive elements (E1 and E4) were fabricated by Jenoptik using a pattern transfer and etch process. Each element is plano parallel Suprasil of high uniformity and surface quality and has fiducials on the center and at 12, 6 and 9 o'clock positions to facilitate alignment in decenter and clocking. The E2 and E3 elements were fabricated by Optimax of Rochester, New York again of Suprasil material. The surfaces on E2 and E3 are all spherical, concave on one side and convex on the other with varying degrees of wedge and different radii of curvature. The E2 and E3 element radii and surface figure were measured prior to delivery to NASA. The E2 and E3 elements are also fiducialized with center and edge fiducials to enable alignment. In addition, the E2 and E3 elements have integral flats on the bottom edge and on one side edge, which are related to the assembly's optical axis. Optimax placed the fiducials and integral flats to tolerances specified in the element drawings with tighter knowledge than placement requirements. Figure 4 shows the fiducials and integral flats used on E2 and E3.

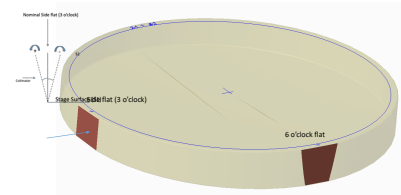


Figure 4. E2, E3 Fiducias and integral flats

2.3. Grism Element Testing

Testing of each grism substrate at the vendor was only performed on each surface using interferometry at 632.8 nm wavelength. Acceptance testing of each grism element was performed at NASA Goddard at 1550 nm wavelength using computer generated holograms (CGH) and a ZYGO interferometer³. The CGH's were designed specifically for each element and fiducialized to allow deterministic alignment of the elements to each CGH to avoid "aligning" out fabrication errors. Careful attention was placed on utilizing high quality CGH substrates as many vendors are now recycling substrates. Element fiducials and integral flat alignment knowledge was transferred to cube and SMR references on temporary mounts to allow accurate

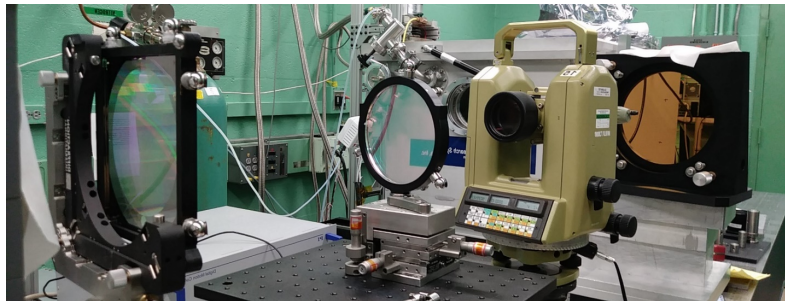
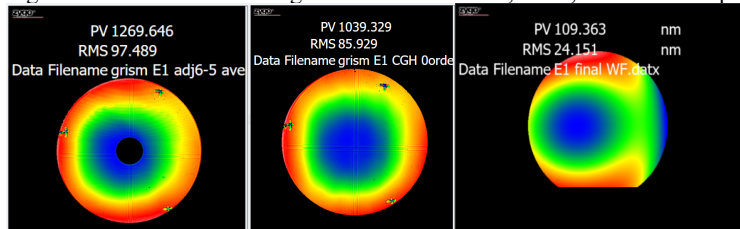


Figure 5. E1 CGH Test Configuration and E1+CGH, CGH, E1 wavefront plots



placement of the elements in 6-degrees of freedom relative to the CGH. The CGH's were designed to operate in collimated space and were tilted 10 degrees with respect to the interferometer's optical axis to avoid ghosts. The placement of the CGH with respect to the ZYGO instrument was determined with laser tracker and a theodolite. A retro flat was used behind the optic under test to create a double pass cavity. Each CGH and reference flat cavity was then subtracted out to determine the element transmitted wavefront error. The test configuration for E1 and the measured wavefront maps of the CGH+E1, CGH alone and processed E1 are shown in Figure 5. Each element was then characterized and compared to the expected WFE. With the exception of the power term for E2 and E3, all elements were determined to be within specification. The discrepancy in power for E2 and E3 was due to a CGH design mismatch, as the EDU elements were changed from fused silica to Suprasil. Modeling was performed to determine if this would have an impact on the assembled grism performance; since Element 2 and Element 3 have opposite power it was determined that the majority of the error would be compensated in the assembly.

2.4. Grism Alignment and Wavefront Error Budget

The grism fabrication and alignment budget is based on an analysis of proposed reasonable tolerances for fabrication from discussions with Optimax and alignment from previous experience on other NASA programs. Simulations of the alignment were performed that indicated that we should be able to achieve our required wavefront performance with these tolerances and a final compensation step. The opto-mechanical alignment budget for each grism element is shown in Figure 6. We were confident that the alignment would be stable during cooldown and allocated reasonable tolerances that allowed us to meet requirements. We based this on prototype testing and modeling of the grism elements in their invar mounts, which are closely matched in coefficient of thermal expansion (CTE). There were still unknowns as to the changes in figure due to coatings on the optics and other cooldown effects. The grism wavefront error budget requires grism performance across the field of view to be less than 90 nm transmitted RMS wavefront error at the operating temperature.

PARAMETER	ALIGNMENT	
	Tolerance	(units)
Decentering, Horiz. (u-axis)	0.100	mm
Decentering, Vertical (w-axis)	0.100	mm
Focus (v-axis)	0.050	mm
Tilt, Horizontal (u-axis)	0.250	mrad
Tilt, Vertical (w-axis)	0.250	mrad
Tilt, axial (clocking, v-axis)	0.500	mrad

Figure 6. Alignment Budget

2.5. Grism element alignment and bonding

The grism mechanical design is an evolution of the prototype grism, which allowed for tip/tilt despace adjustment between element cells using spherical washers and shims and repeatability of decenter of each cell in the assembly using alignment bushings. The fused silica elements in the prototype were aligned in the invar cells and then bonded in place at three flexure positions to minimize cooldown distortion. The EDU grism mechanical design was modified to allow each element to be aligned deterministically to the grism mount coordinate system and then bonded in place, achieving superior initial alignment. E2, E3 and E4 were individually alignment to the grism mount coordinate system on a hexapod using a Micro-Vu non-contacting coordinate measuring machine to measure the position of the element in decenter and despace. The process is shown in Figure 7; the element is installed in a hexapod protruding through the grism mount, theodolites (a) were used to view the integral flats on the elements to guide the hexapod (b) adjustment to align each element in tip/tilt and clocking. Once the element was aligned in 6-degrees of freedom, the mechanical cell was slipped over the element (c) using the guide bushings to register the cell to features on the grism deck. The spherical washers and nominal shims were in place during this process. Once the cell was in place the optic was bonded (d) at three positions to the flexures using a 2-step process. First a plunger was bonded to the element edge, after a curing period the plunger was then bonded to flexures on the cell; in this way we eliminated strain to the optic due to epoxy shrinkage. After the epoxy cured, E2 was removed and the process repeated for E3. E4 has a flat surface and therefore did not require integral flats. Instead a fold mirror was positioned over it and the normal to the fold and the E4 beam was acquired with theodolites and adjusted to the nominal tip/tilt angle. The element was then adjusted in clocking, decenter and despace using the Micro Vu and rechecked with the theodolite prior to bonding it in its cell. The final element, E1 was aligned in a similar fashion and bonded directly to the grism deck/mount. E1 is bonded last because once it is in place the hexapod cannot access the space where E2, E3 and E4 reside. Each cell and the grism deck are fit with alignment cubes, which were measured at each stage of element alignment to provide a reference to ensure that each cell was repeatably aligned back to its original position during grism assembly. We found that we could achieve about 0.25 milliRadians of repeatability and accuracy of adjustment with our spherical washer/shim stack.

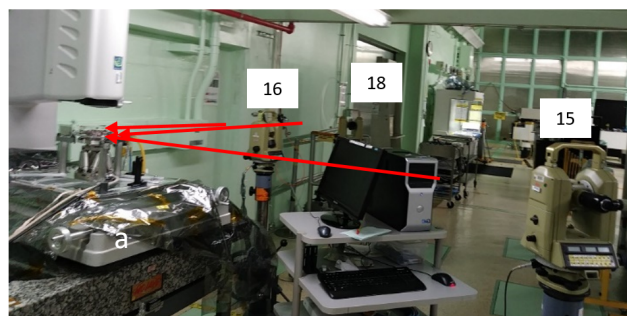
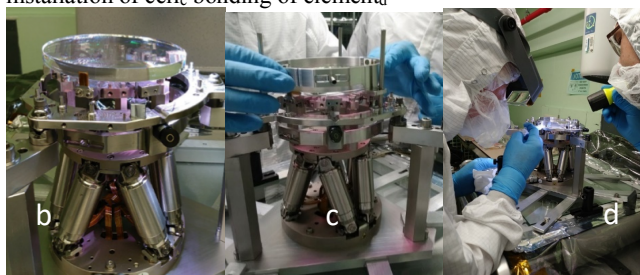


Figure 7. E2 Alignment_a to Grism Mount using hexapod_b, installation of cell_c bonding of element_d



We found that we could achieve about 0.25 milliRadians of repeatability and accuracy of adjustment with our spherical washer/shim stack.

2.6. Grism ambient testing

The WFIRST Wide Field Channel has an exceptionally large field of view, which creates challenges for measuring the performance of the grism at the assembly level. In the flight configuration the grism is at the exit pupil of the WFIRST telescope situated after the tertiary but resident in the WFI as shown in Figure 8. In order to test the grism, we developed an approach whereby the grism was placed on a

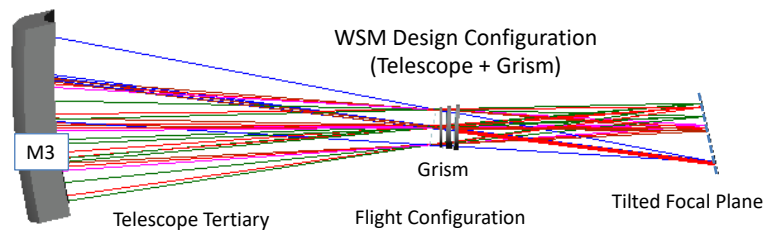


Figure 8. Grism Flight Configuration vs Test Configuration

hexapod and tilted relative to an interferometer to allow the characterization of the wavefront at discrete fields. Unlike the grism configuration of the grism relative to the telescope, where the grism is fixed and the source varies by field. During wavefront measurements, we used a ZYGO Verifire wavelength shifting interferometer, which operates at 1550 nanometers, near the center of the grism wavelength range, which spans 1000 to 2000 nanometers wavelength. Figure 9 shows the test configuration, which requires the grism to be tilted over a 20 x 14-degree range in azimuth and elevation.

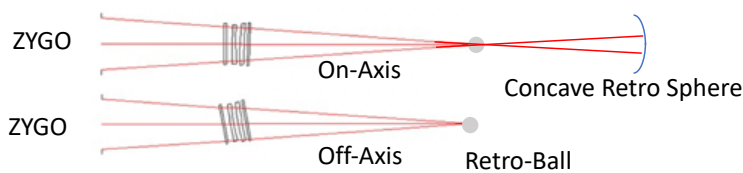


Figure 9. Grism test configuration

In this test configuration, the focal surface sweeps out a curve instead of an essentially flat focal surface when it is used with the WFIRST telescope. We defined a test coordinate system by first installing a 6-inch transmission sphere into the interferometer and internally aligning it. Then we align a retro ball as the focus of the transmission sphere to set the zero the nominal desired focus of the system. We swap out the transmission sphere and install a transmission flat on the interferometer to establish the boresight of the system. Co-boresight of the transmission flat and transmission sphere was separately verified (we had to select a transmission flat that had a small wedge angle). The grism was then installed on the hexapod and the front surface of E1 was aligned to the transmission flat in tip/tilt to achieve a null and place the E1 normal on the optical axis of the interferometer as shown in Figure 10. The grism was then centered to the test beam by aligning the E1 center fiducial to the interferometer center fiducial. The transmission flat is then replaced by the f/7.2 transmission sphere and internally aligned to the interferometer. A laser radar is used to acquire the grism reference targets that have been characterized relative to the grism coordinate system on the micro-vu. The laser radar also acquires the retro ball that was placed at the focus of the transmission sphere prior to the introduction of the grism. The test coordinate system is established by using the on-axis grism position that defines the boresight of the test frame, which has its origin at the retro ball. The grism is then translated along the optical axis to place it at the nominal distance from the retro ball using the hexapod, while maintaining centration to the ZYGO beam. The initial retro-ball position and 6 degree of freedom placement of the grism relative to the ZYGO defines the on-axis reference position to which all other measurements are related. This position is transferred to tie points on the optical table to provide a set test reference frame. The retro-ball is then translated to null power and the position of the retro-ball measured using the laser radar. The grism is designed to be zero power

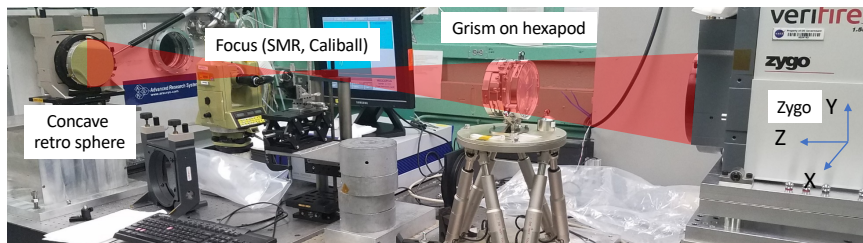


Figure 10. Grism configuration – interferometer on right, grism in center on hexapod and retro-caliball and concave retrosphere on left

at the nominal spacing to the focal surface, therefore a translation of the retro-ball represents the error in the back focal length (BFL) of the grism on-axis. A caliball was used as the retro-ball to determine the back focal length and confocality for the on-axis and off-axis field points. Transmitted wavefront measurements were made by removing the retro-ball and aligning a large concave retro-sphere to null the beam to the interferometer. ZYGO recommends a ratio of 5:1 to 10:1 of the transmission element to the retro-sphere to minimize

retrace error in the measurement. For the wavefront measurements concave retro is better suited for the measurement because the Caliball use would also require multiple measurements be taken at different rotations of the caliball to average out surface irregularities. Modeling of the test configuration was performed to determine nine field points that could be used to determine the performance of the grism over a representative field of view. The model also provided the nominal position of the retro-ball relative to the on-axis position for each field. It is important to have this information to determine the offset of each field's focus point from nominal as this is a measure of the confocality of the grism across the field, due to the design residual, element alignment and figure error of each element. Residual focus error for each field cannot be compensated as the telescope and WFI focus is set for the imaging mode through the filters. Figure 11 shows the test field points in degrees of physical tilt off-axis and wavefront map for these fields. The hexapod was adjusted in tip/tilt to interrogate the wavefront error at nine field positions relative to the on-axis test frame. Initial measurements of the grism were performed over fields F1-F5 to provide guidance for optimization using E2. Our strategy was to balance the x and y astigmatism at fields F4, F5 and F2, F3 by adjusting E2 in tip and tilt using sensitivities provided by modeling. Once the astigmatism was balanced, we measured the error in the back focal length and shimmed E2 to maintain tip/tilt and provide the calculated despace for back focal length correction. We then measured the wavefront error at F1-F5 using the hexapod to adjust tip/tilt and the concave retrosphere configuration. Figure 12 shows the initial wavefront resulting from the opto-mechanical alignment and the corrected wavefront at all nine fields after compensation by E2 adjustment. The wavefront plots are generated from the measured Zernike terms and do not display pupil mask in the grism assembly. The central obscuration required us to

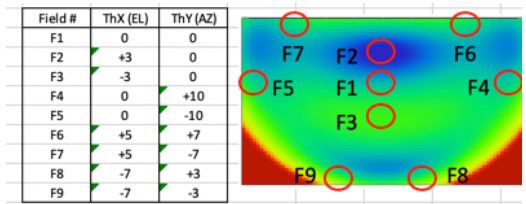


Figure 11. EDU Grism test field points (degrees)

use 6th order Zernike Fringe fits of the data (vs 12th order) in order to avoid a false fit of spherical aberration. The residual asymmetry in the F2,F3 and F4,F5 fields was due to non-repeatability in the spherical washer stack on the grism mount, which will be corrected in the flight model grism. Back focal length error and confocality were determined by using laser radar and adjusting the retro-ball to null power at each field position. We did not correct the back focal length error of -72 microns at the end of optimization as we expected that a despace adjustment of the grism E2 may be required after measurements at cryogenic operating temperature. When the focus is biased for the average back focal length, the confocality is 18 to -35 microns across the field, which is near the error of the measurement for the geometry of a laser radar measurement. The goal for the flight grism is to set the on-axis back focal length to within 30 microns, which would allow compensation by despacing the grism assembly by 1 mm in the pupil wheel.

use 6th order Zernike Fringe fits of the data (vs 12th order) in order to avoid a false fit of spherical aberration. The residual asymmetry in the F2,F3 and F4,F5 fields was due to non-repeatability in the spherical washer stack on the grism mount, which will be corrected in the flight model grism. Back focal length error and confocality were determined by using laser radar and adjusting the retro-ball to null power at each field position. We did not correct the back focal length error of -72 microns at the end of optimization as we expected that a despace adjustment of the grism E2 may be required after measurements at cryogenic operating temperature. When the focus is biased for the average back focal length, the confocality is 18 to -35 microns across the field, which is near the error of the measurement for the geometry of a laser radar measurement. The goal for the flight grism is to set the on-axis back focal length to within 30 microns, which would allow compensation by despacing the grism assembly by 1 mm in the pupil wheel.

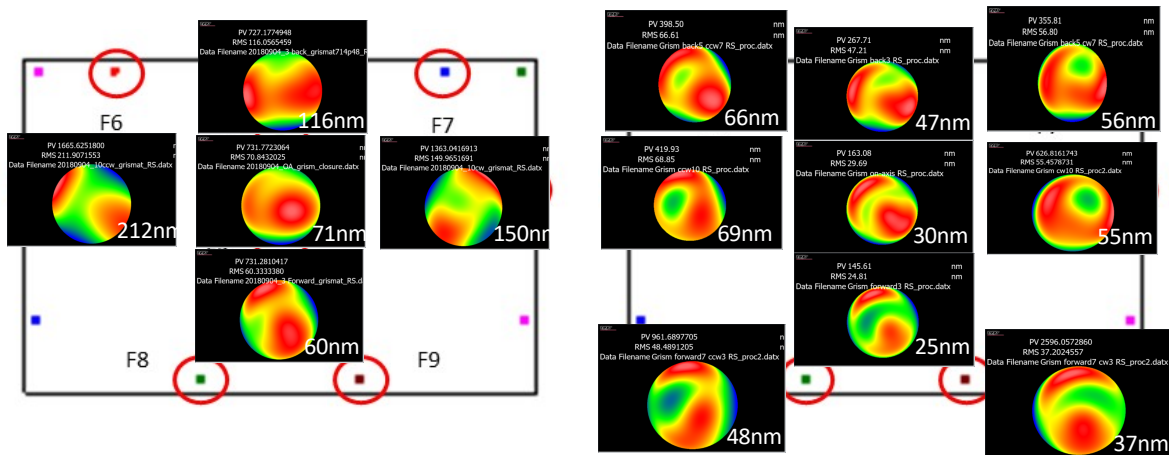


Figure 12. Initial and adjusted wavefront error of grism

2.7. Grism cold testing

The grism design is athermalized in that the CTE of Suprasil very closely matches the CTE of the invar mechanical cells, mount and adhesive. The bond thickness is approximately 125 microns to minimize the strain due to the epoxy CTE after cooldown to the operating temperature of 170 Kelvins. The grism was tested in the Cryogenic Displacement Monitor Facility (CDMF); which is specially designed to support optical testing. The CDMF has a 2-stage cryo cooler and cryo pumps that allow it to be cooled as low as 37 Kelvins. It is also fitted with four large ports to enable optical testing. Each port has a high-quality glass pressure window and two sapphire windows, one is thermally sunk to the first stage cooler and shroud and the other to the second stage cooler and inner shroud. This cools the sapphire windows to prevent heat loading of the item under test. The test configuration for the grism cold test is shown in Figure 13. The ZYGO beam shown in Figure 13, goes through the CDMF windows, the grism and then retro reflects off of either a caliball or a convex retrosphere (CVR). The length of the CDMF precluded the use of the concave retrosphere, the CVR allowed the cavity to fit within the chamber. The caliball and CVR are on a three-axis stage to allow realignment of the caliball or CVR after cooldown. The CVR is used for wavefront measurements while the caliball is used for back focal length and confocality measurements. The confocality metrology was performed using the laser tracker with the CDMF lid open to place the caliball and the grism in the test coordinate frame for the field being tested. When the CDMF lid was closed, measurements of the grism to caliball alignment were collected using a laser radar through the back CDMF window. From previous programs we have learned that laser radar measurements through a window have to be corrected analytically for phase errors⁴. However, for measuring small changes in alignment, that is relative changes of less than 1 mm; we demonstrated that the laser tracker and laser radar correlated to about 23 microns. Therefore, we did not need phase corrections on the laser radar measurements during our cold test. We do not have a cryogenic hexapod and the space within the CDMF is limited, therefore, we could only test one field point at a time without performing a chamber break. The grism is on a translation stage to allow it to be moved out of the ZYGO cavity to the CVR. This allows a measurement of the window and CVR wavefront (reference cavity); which is subtracted from the grism measurement (through the window and off of the CVR) during data processing. The alignment steps are as follows:

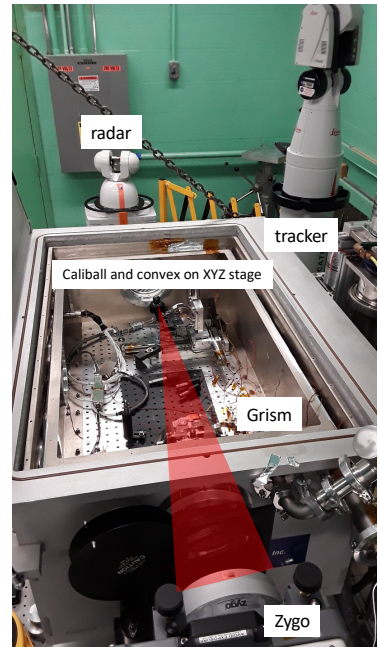


Figure 13. Grism in CDMF

The alignment steps are as follows:

1. With the CDMF lid open, align a 1" SMR to the ZYGO and null power, record its position relative to table tie points using the Laser Tracker and the Laser Radar (the caliball and SMR are swapped depending on if the laser radar or laser tracker are doing the measurement)
2. Replace the ZYGO transmission sphere with the transmission flat
3. Translate the grism into the beam and align it in tip/tilt and centration to the transmission flat
4. Adjust the grism in despace to the nominal spacing to the SMR using the laser tracker
5. Establish the on-axis CDMF frame with both laser radar and laser tracker (there are also tie points in the CDMF)
6. Replace the transmission flat with the transmission sphere
7. Acquire the grism wavefront (without adjusting the caliball)
8. Translate the caliball to null power and measure the position of the caliball/SMR with laser tracker and laser radar
9. Translate the CVR into the beam and null it to the grism
10. Acquire the wavefront of the grism
11. Translate the grism out of the reference cavity
12. Acquire the wavefront of the reference cavity (subtract the reference cavity from the grism + reference cavity and compare to the wavefront outside of the CDMF)
13. Translate the grism back into the reference cavity and remeasure (repeatability check)
14. Close the CDMF chamber and pump it down to 10⁻⁶ Torr

15. Cooldown the grism to 160 Kelvins
16. Realign the CVR to the grism and measure the wavefront (measure the CVR and Grism with laser radar)
17. Translate the grism out of the reference cavity
18. Measure the reference cavity (subtract to get the cold grism WFE)
19. Align the caliball to the reference cavity and measure with laser radar
20. Translate the grism back into the reference cavity
21. Check the alignment of the grism to the caliball and tie points
22. Null the caliball to the grism and measure with the laser radar to get the cold back focal length
23. Warm up and perform the same steps to get the warm WFE and BFL

Characterization of the grism at cold temperature is a time consuming and difficult process and requires about a week to complete during the one cold cycle per field point. We measured the wavefront at three different field points at cold operating temperature of 160 Kelvins. For the three fields that were measured the change in the RMS wavefront

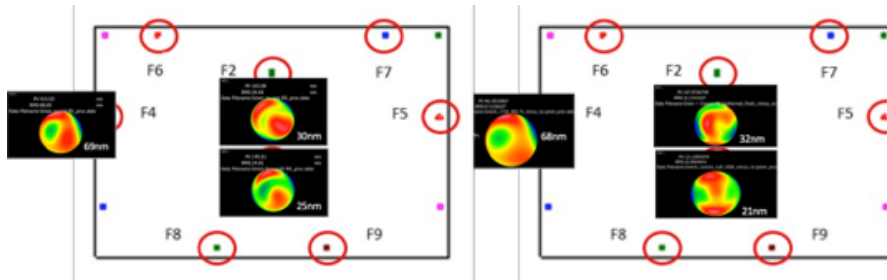


Figure 14. Ambient and Cryogenic Wavefront map of EDU Grism

error after subtraction of the reference cavity was in the noise of the measurement. Visually the wavefront plots look very similar, the Zernike fringe terms are however larger than the RMS error difference would indicate. Our metric for success is RMS wavefront error, therefore we believe

the grism has been proven meet our requirements for cooldown. This can be seen in Figure 14. Development of the process for measuring the back focal length was a refinement that was only implemented on the on-axis field point. Modeling indicates that the grism should remain confocal when cold and the negligible change measured in wavefront error supports that conclusion. The confocality for the Flight Unit grism will be measured at several field points to verify confocality. Figure 15 shows the results of the back focal length measurements of the grism performed before cooldown, at cold temperature and after warmup. The ambient vacuum measurement in the chamber agrees with the out of the chamber measurement to within -19 microns. The change from ambient to cold is +37 microns and the change from cold back to ambient is -9 microns. The difference from warm pre-cooldown to post-cooldown is -28 microns and agrees with the out of chamber measurement to +9 microns. We believe that all of these deltas are within the 2-sigma statistical error in the measurement (± 23 -micron correlation was demonstrated for small alignment changes, between laser radar through the CDMF window and laser tracker at ambient). Based on this test, we would align for nominal BFL at ambient temperature and pressure. There are however, other considerations as the EDU grism does not have the out-of-band coating on E2. The out of band coating is comprised of over 100 layers, and was applied on the spare E2 optic by Alluxa in parallel with EDU testing. We determined that the transmitted wavefront error due to the coating strain was less than our allocation of 16 nm in ambient conditions. The EDU E2, will be replaced by the coated E2, upgrading it to an Engineering Test Unit (ETU). The grism will then be reoptimized and tested across the FOV at ambient and at select fields at cold temperature to demonstrate that the coating does not degraded the transmitted wavefront error beyond its allocation or require adjustment to BFL.

On-Axis		x mm	y mm	z mm
Ambient Vacuum				
Focus (w/ grism)	Caliball	-0.833	-0.529	715.140
Focus (no grism)	Caliball	-0.837	-0.409	715.231
	Delta (mm)	0.004	-0.120	-0.091
Cold Vacuum				
Focus (w/ grism)	Caliball	-0.786	-0.501	715.339
Focus (no grism)	Caliball	-0.824	-0.403	715.393
	Delta (mm)	0.038	-0.098	-0.054
			cold - warm	0.037
Post Test Ambient Vacuum				
Focus (w/ grism)	Caliball	-0.785	-0.550	715.204
Focus (no grism)	Caliball	-0.845	-0.423	715.267
	Delta (mm)	0.060	-0.128	-0.063
			warm-warm	0.028

Figure 15. Ambient to Cold BFL change of grism

3.0 SUMMARY AND FUTURE WORK

The NASA GSFC WFIRST grism team has demonstrated the ability to design, procure, align, test and maintain the alignment of the optical elements of the EDU grism to produce excellent wavefront performance across its large field of view. The wavefront error and back focal length change from ambient to cold operating temperature is within the measurement error validating its athermal design. Initial testing of the EDU grism spectral resolution, diffraction efficiency and dispersion, indicates that it will meet its functional requirements as a slitless spectrometer.⁵ The EDU will be upgraded to an Engineering Test Unit (ETU) once the E2 element is changed out for an E2 element with the bandpass coating and the grism alignment reoptimized. The ETU wavefront will be tested over 9 field points in ambient conditions and at select fields at cold temperature to look for coating induced changes relative to the EDU. ETU spectral performance will be measured over multiple fields in ambient conditions and on-axis at cold operating temperature at the grism level of assembly. The flight grism design is being optimized based on the EDU and further maturation of the WFIRST telescope design. In order to gain additional performance margin for the flight design and further reduce packaging, the E1 and E2 diffractive surface designs are being modified and etched on both sides of a single new E1 element. Extensive modeling and Monte Carlo analysis of the new 3-element grism indicates equivalent or superior performance with the new design. The EDU has served as a valuable tool in the development of both the grism design and the evolution of alignment and test procedures required to meet and verify its challenging wavefront criteria.

REFERENCES

- [1] Content, D., et al. "Wide-Field InfraRed Survey Telescope (WFIRST) 2.4-meter mission study." SPIE UV/Optical/IR Space Telescopes and Instruments: Innovative Technologies and Concepts VI. San Diego: SPIE Proceedings, 2013. 7.
- [2] Gong, Qian, et al. "Wide-Field InfraRed Survey Telescope (WFIRST) slitless spectrometer: design, prototype and results." Space Telescopes and Instrumentation: Optical, Infrared, and Millimeter Wave. Edinburg: SPIE, 2016. 18.
- [3] Dominguez, M., et al. "Infrared Testing of the Wide-Field InfraRed Survey Telescope grism using Computer Generated Holograms" Design and Fabrication Congress 2017 (IODC, Freeform, OFT) © OSA 2017
- [4] Hayden, J., et al. "Mathematical Corrections Applied to Laser Radar Measurements Made through a Cryogenic Vacuum Chamber Window" CMSC Conference, Volume 6, Issue 2, September, 2011
- [5] Gong, Qian, et al. "Spectral and Radiometric Calibration of WFIRST Slitless Spectrometer (grism)" SPIE UV/Optical/IR Space Telescopes and Instruments: Innovative Technologies and Concepts IX: San Diego: SPIE Proceedings, Aug 2019